ISSN 1330-3651 (Print), ISSN 1848-6339 (Online)
Received: 21 November 2024; Accepted: 24 August 2025

https://doi.org/10.17559/TV-20241121002148
Original scientific paper

Power Ripple Reduction in Cascade Boost Converters Using PI-Based MPPT Control for Solar Cells

Sude KART

Abstract: It is crucial to operate PV panels at maximum power due to their low power generation capabilities. There are various types of control methods referred to as MPPT (Maximum Power Point Tracking) algorithms. Among these, the ES (Extremum Seeking) control algorithm, which is a type of MPPT algorithm that provides fast response in nonlinear systems, is used in this study. However, high ripples occur in the output power of the PV system operated at the maximum power point using the ES algorithm. These ripples negatively affect the performance and lifespan of the PV panel and also increase the switching cost in the converter fed by the PV panel. To overcome these drawbacks, in this study, the classical ESC (Extremum Seeking Control) method has been positively enhanced. The developed new controller is simulated in the Matlab/SIMULINK environment in a system consisting of a DC-DC cascade boost converter and PV panel. According to the obtained results, it is observed that the proposed controller reduces the power ripples existing in the standard ES control and provides a more stable and efficient operation of the PV system.

Keywords: boost converter; extremum seeking control; PI controller; PV panel

1 INTRODUCTION

With the increasing energy demand, studies on renewable energy sources have gained momentum in recent years [1]. Solar energy, one of these renewable energy sources, is preferred more than others in our country due to its geographical location and decreasing PV panel prices. However, the efficiency of PV panels, which still does not exceed 20%, is a significant issue [2]. The output voltage of a photovoltaic (PV) panel can be increased using a boost-type direct current-direct current (DC-DC) converter (Fig. 1). The choice of converter significantly affects the efficiency of the system. Various DC-DC converters are available, such as flyback, full bridge, half bridge, buck, and boost converters [3]. Each type has its own advantages and limitations. For the specific purpose of boosting the PV panel's output voltage, a boost converter is the most suitable choice. To achieve a high output voltage with a standard boost converter, a high duty cycle is required. However, operating with a high duty cycle can negatively impact the converter's performance. To maintain a high voltage ratio while avoiding excessively high duty cycles, a cascade DC-DC boost converter can be employed [4].

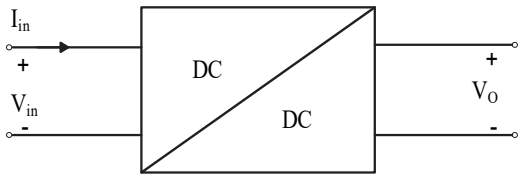

Figure 1 DC-DC converter block diagram

The ability of a PV panel to generate electrical power is limited and the applied current or voltage varies non-linearly. Therefore, PV panels are operated at maximum power [5]. There are many maximum power operation algorithms [6, 7]. The most popular MPPT algorithm due to its simplicity and ease of implementation is the P&O method [8]. This algorithm is based on calculating the change in power by sampling the current and voltage of the PV panel [9]. The P&O algorithm operates by periodically increasing or decreasing the PV panel voltage, thus causing the system to oscillate around the MPP [10]. However, P&O can exhibit unstable behavior in rapidly changing environments [11]. Since PV is a nonlinear source that varies with radiation and temperature, it may be preferable to use extremum seeking control, which provides a faster response instead of the P&O algorithm. Because extremum seeking control is an adaptive nonlinear control method, it can be successful when the control converges. Another advantage is that extremum seeking control does not require prior knowledge of the PV.

In reviewing the literature on optimizing photovoltaic (PV) systems for maximum power, various methods have been explored. Hussain Basha and Rani explored various traditional Maximum Power Point Tracking (MPPT) methods, including Variable Step Size Perturb and Observe (VSS-P&O), Modified Incremental Conductance (MIC), and Fractional Open Circuit Voltage (FOCV) [12]. They also evaluated several soft computing MPPT approaches, such as Fixed Step Size Radial Basis Function Algorithm (FSS-RBFA), Variable Step Size Radial Basis Function Algorithm (VSS-RBFA), Adaptive Fuzzy Logic Controller (AFLC), Particle Swarm Optimization (PSO), and Cuckoo Search (CS), offering detailed comparisons to assess their effectiveness with different converter configurations.

Shaw proposed an analog MPPT method for battery charging systems utilizing a DC-DC boost converter, focusing on robustness and fast dynamic performance [13]. His study applied nonlinear dynamics and bifurcation theory to design an MPPT system capable of adapting to rapidly changing conditions, demonstrating both theoretical and practical validation through prototype testing.

Zdiri and colleagues compared the dynamic behavior of different MPPT techniques, including P&O, Fuzzy Logic Controller (FLC), Artificial Neural Network Proportional-Integral (ANN-PI), and ANN-Swarm Method (ANN-SM) [14]. Their results showed that the ANN-SM controller could quickly reach the maximum power point (MPP) across varying conditions and exhibit lower power fluctuation rates compared to P&O. The

YSA-SM algorithm was found to be more efficient in terms of energy consumption.

Siddique and his team introduced an effective Incremental Conductance (IC) algorithm for grid-connected PV systems [15]. Their approach aimed to optimize PV array parameters to ensure effective matching with DC/AC converters, focusing on achieving optimal values for components such as inductors, capacitors, and boost converter duty cycles. Their study provided a thorough analysis of MPPT techniques and detailed design considerations for PV converter systems.

However, the maximum point in the Maximum Point Search algorithm changes depending on changing conditions [16]. Therefore, large fluctuations occur in the output power. These fluctuations also reduce the performance and lifespan of the PV panel. Additionally, they increase the switching cost in the converter fed by the PV panel. There are some studies in the literature to reduce these ripples. Firdaus and his team implemented Maximum Power Point Tracking (MPPT) using the Fuzzy Logic-Particle Swarm Optimization (FL-PSO) approach [17]. They employed FL-PSO to locate the Maximum Power Point (MPP) and reduce power output ripples from the photovoltaic system. Their results showed that the FL-PSO method significantly outperforms the Particle Swarm Optimization (PSO) method, providing faster convergence and better performance.

In a separate study, Vaigundamoorthi and colleagues analyzed the control of chaotic dynamics in a solar PV system equipped with a SEPIC DC-DC converter [18]. The SEPIC converter, known for maintaining continuous input inductor current, enables comprehensive scanning of all *I-V* curves from open-circuit voltage (V_{oc}) to short-circuit current (I_{sc}). The researchers focused on ensuring stable output voltage and minimizing oscillations near the MPP.

Additionally, Brunton et al. (2010) developed a ripple-based extremum seeking control method that reduced output ripple and achieved over 99% tracking efficiency in PV systems [19]. Zazo et al. (2012) used a Newton-like ESC approach to provide more stable transient responses and lower ripple levels compared to conventional ESC [20]. Ghaffari&Krstić (2014) introduced a multivariable Newton-based ESC algorithm demonstrating faster convergence and reduced ripple regardless of environmental variations [21]. In simulation work, Chellakhi et al. (2022) achieved up to six-fold reduction in boost converter ripple amplitude (both input and output) compared to conventional INC MPPT [22]. These studies reinforce the validity and effectiveness of the proposed PI-based ESC controller. However, despite these advances, none of the above approaches explicitly integrate PI control within an ESC framework for the specific purpose of minimizing power ripple in PV systems, nor do they present comprehensive validation under varying conditions, as done in this study.

In this study, an improved Extremum Seeking Control (ESC) method was proposed to reduce power ripples. This new controller was simulated in a Matlab/SIMULINK environment with a PV panel and a DC-DC cascade boost converter. The simulation results highlighted the enhanced performance of the proposed controller compared to the traditional ESC method. While PID or other classical control methods are generally used in the literature, PI-based ESC control is applied in this study. This innovative approach contributes to the development of MPPT techniques by increasing the diversity of control methods.

2 MODELING AND ANALYSIS

2.1 Solar Panel

A solar panel cell consists of a *p-n* semiconductor junction that generates direct current (DC) when exposed to light. The amount of current produced is directly proportional to the intensity of the solar radiation. In the absence of light, the solar cell does not produce any current [23]. The equivalent electrical circuit of an ideal solar cell is illustrated in Fig. 2.

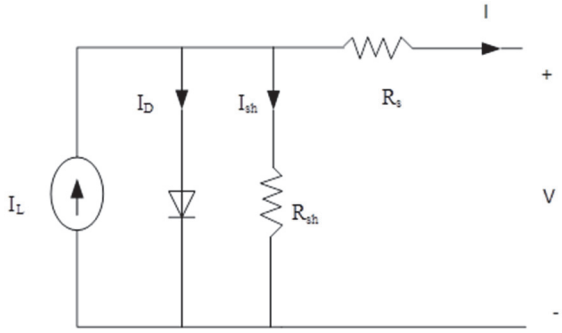

Figure 2 Equivalent electrical circuit of an ideal solar cell

The current-voltage (*I-V*) graph characteristic of the solar cell is given in Eq. (1);

$$I_D = I_O\left[\exp\left(q\left(V + IR_s\right)/KT\right) - 1\right] \tag{1}$$

The solar cell output current is shown in Eq. (2).

$$I = I_D - I_L - I_{sh} \tag{2}$$

where, I - Solar cell current, A; I_L - Light generated current, A; I_O - Diode saturation current, A; q - Electron charge, 1.6×10^{-19} C; K - Boltzman constant, 1.38×10^{-23} J/K; T - Cell temperature in Kelvin, K; V - Solar cell output voltage, V; R_s - Solar cell series resistance, Ω; R_{sh} - Solar cell shunt resistance, Ω.

2.2 DC-DC Cascade Boost Converter

DC-DC converters are electronic circuits used to increase or decrease the existing voltage level to the desired level. Since converters are nonlinear systems, their efficiency varies depending on the design and control of the circuit. DC-DC converter circuits mainly consist of a power stage and a control stage. The power stage comprises semiconductor circuit elements and filtering elements. It is used to obtain the desired output voltage level depending on the input voltage. The control stage generates the switching signal that activates the semiconductor circuit elements and controls the timing of this signal. DC-DC converters, also referred to as voltage converters or power converters, are classified as boosting (boost), bucking (buck), or buck-boost converters depending on their general purpose [24]. Boost converters

are preferred in applications where high performance is expected despite low output voltage, such as PV systems or fuel cells. In these converters, to obtain high output voltage, it is necessary to keep the duty cycle high. However, selecting a high duty cycle can negatively affect the operation of the converter. One of the proposed solutions to keep the voltage ratio high without increasing the duty cycle too much is to use a DC-DC cascade boost converter [25]. Controlled by a dual-switch structure, this converter consists of two cascaded DC-DC boosting converters. In this case, the output voltage obtained at the first stage is given by Eq. (3).

$$V_{C1} = \frac{V_{in}}{1-d} \tag{3}$$

The output voltage obtained from the 2nd layer of the circuit is given in Eq. (4).

$$V_0 = \frac{V_{C1}}{1-d} \tag{4}$$

The input-output voltage conversion ratio obtained after calculating the voltage values between the layers is given in Eq. (5). d in the equations is the duty cycle of the switch S.

$$V_0 = \frac{V_{in}}{(1-d)^2} \tag{5}$$

In the conducted study, a single-switch DC-DC dual-stage boosting converter was employed with the aim of designing a cost-effective solution by using fewer circuit elements and reducing power losses in dual switching. The output and input voltage calculations for the single-switch circuit are the same as those provided for the dual-switch circuit in Eqs. (3), (4), (5). The circuit diagram of the single-switch DC-DC dual-stage boosting converter is illustrated in Fig. 3.

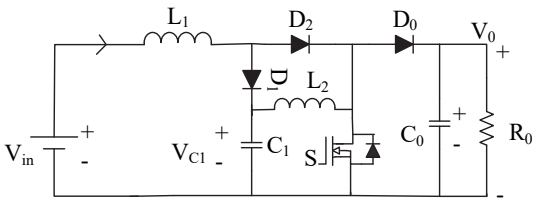

Figure 3 Single switch double stage boost type converter circuit

In the circuit shown in Fig. 3, when switch *S* is closed, diode D_2 is forward-biased, while diodes D_1 and D_0 are reverse-biased. During this phase, the inductor L_1, with current I_{L1}, is energized by the input voltage (V_{in}), and inductor L_2, with current I_{L2}, is powered by the voltage across capacitor V_{C1}. As switch *S* conducts, the currents I_{L1} and I_{L2} flow through their respective paths: I_{L1} through V_{in}, L_1, D_2, *S*, and back to V_{in}, and I_{L2} through V_{C1}, L_2, *S*, and back to V_{C1}. Conversely, when switch *S* is open, diode D_2 becomes reverse-biased, and diodes D_1 and D_0 become forward-biased. During the off period of switch *S*, the energy stored in the inductors flows towards the output RC circuit, establishing the relationship $V_{in} < V_{C1} < V_0$ among the voltages. The currents stored in the inductors decrease gradually during this period [26, 27].

3 MODELLING AND ANALYSIS

3.1 Conventional Extremum Seeking Controller

The ES control is an adaptive MPPT method. The ES control scheme can be represented as shown in Fig. 3. This controller adapts based on the slope of the power curve, maintaining stability across different operating conditions [19, 28]. It works by introducing a perturbation signal asin (ωt) into the input u, which helps determine the optimal value for *u*. This perturbation causes a corresponding change in the power output. The control variable U_{np}, which is derived by high-pass filtering the power, is demodulated to indicate deviations from the Maximum Power Point (MPP): positive for deviations to the right and negative for deviations to the left. By integrating this demodulated signal and adjusting the parameters accordingly, the controller adaptively regulates *uuu* to effectively track the MPP [30].

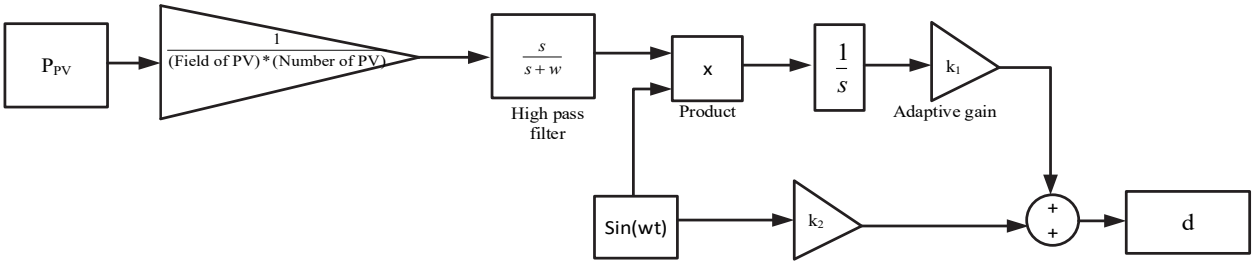

Figure 4 Schema of extremum seeking control

The performance of the control system is influenced by the choice of system parameters. Specifically, the frequency of the periodic sinusoidal perturbation signal (ω) and the cut-off frequency of the high-pass filter (ω_h) play crucial roles in this selection process.

$w >> w_h >>$ The dynamic speed of the controlled PV

The mathematical representation of the block diagram in Fig. 4 is as in the equation below.

$$\sin wt\left[\frac{P}{(\text{field of PV})(\text{number of PV})}\frac{1}{s+\pi}k_1 + k_2\right] = d \tag{6}$$

3.2 Improved Extremum Seeking Control

The developed method is a PI-based ES control method. The PI controller and the ES controller are

cascaded in series. Thus, the aim is to make the ES control more efficient with the advantage of the PI controller.

The mathematical expressions of these two controllers are combined to obtain the mathematical representation as shown in Eq. (7). The block diagram representation of this enhanced controller can be drawn as depicted in Fig. 5.

$$\frac{20\left[\sin wt\left(\frac{P}{(\text{field of PV})(\text{number of PV})}\frac{1}{s+\pi}k_1+k_2\right)\frac{I_{PV}}{28}\right]}{1+\frac{200}{s}} = d \quad (7)$$

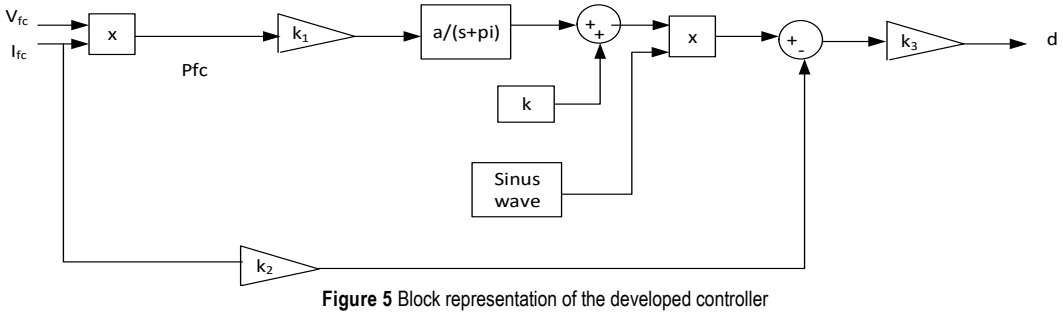

Figure 5 Block representation of the developed controller

In this study, the PI controller parameters were tuned using an iterative, trial-and-error approach. The primary objective was to reduce output power ripple while achieving a fast settling time. To this end, different combinations of proportional (K_p) and integral (K_i) gains were tested within practical limits until the system met the desired transient and steady-state performance criteria. While well-known tuning methods such as Ziegler-Nichols and Cohen-Coon were initially evaluated, they proved unsuitable for this application because photovoltaic (PV) systems exhibit nonlinear and time-varying behaviour [31, 32]. These classical methods generally assume linear, time-invariant dynamics, which can result in poor performance or even instability in PV-fed boost converter systems. For these reasons, a simulation-driven trial-and-error process was chosen, enabling adjustments that reflect the nonlinear characteristics and environmental variability of the system. The final K_p and K_i values were determined to provide the best balance between ripple suppression, rapid tracking of the Maximum Power Point (MPP), and overall system stability.

4 RESULTS FOR SIMULATION AND DISCUSSIONS CONCLUSION

The block representation of the entire proposed system is shown in Fig. 6.

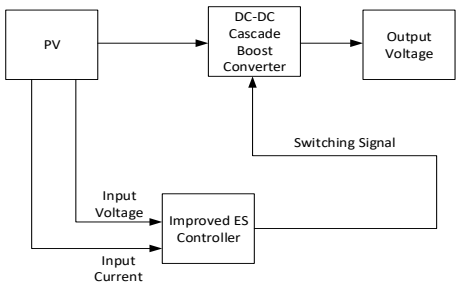

Figure 6 Block representation of the entire proposed system

The current-power (*I-P*) graph of the input of the system, that is, the output of the PV panel, is as shown in Fig. 7. As the *I-P* graph searches for the maximum power, it spirals around the maximum power. The faster it finds the maximum power, the sparser this spiral will be.

Fig. 8 shows the change of PV power over time.

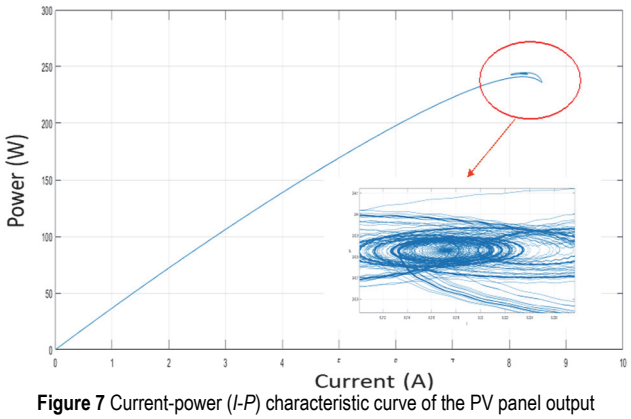

Figure 7 Current-power (*I-P*) characteristic curve of the PV panel output

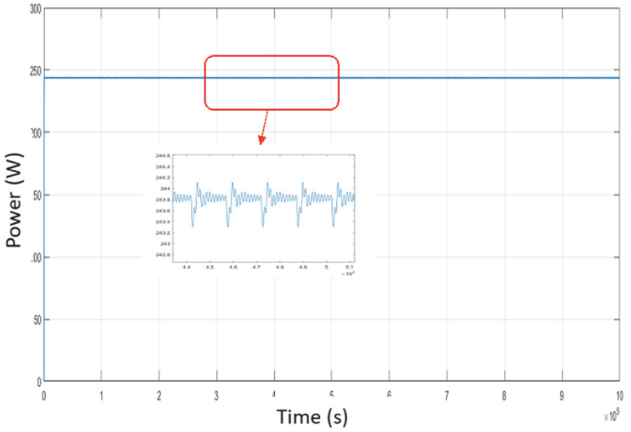

Figure 8 Graph of PV power variation over time

The parameters of proposed converter are given in Tab. 1.

Table 1 The parameters of the converter

Input voltage	30-60 V
Output power	245 W
Inductance	50 µH
Capacitor	220-470 µF

The current-power (*I-P*) graph of PV controlled with the proposed controller is as shown in Fig. 9. As seen in Fig. 9, the spiral motion around the maximum power is more sparse compared to Fig. 7.

The change of PV power over time in the system with the proposed controller is given in Fig. 10.

The current-power (*I-P*) graph of the PV for the radiation values S = 1000 and s = 600, controlled by the proposed controller, is as shown in Fig. 11.

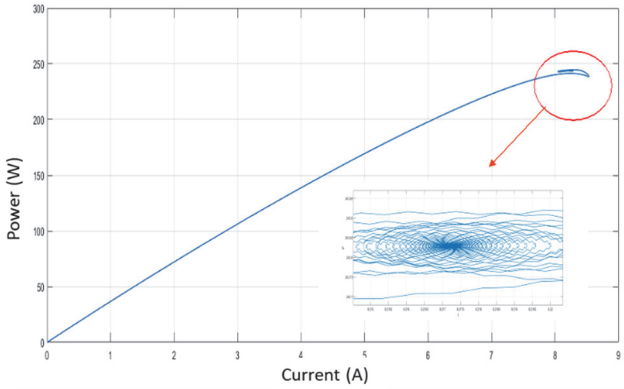

Figure 9 Current-power (*I-P*) characteristic curve of the PV system under the proposed controller

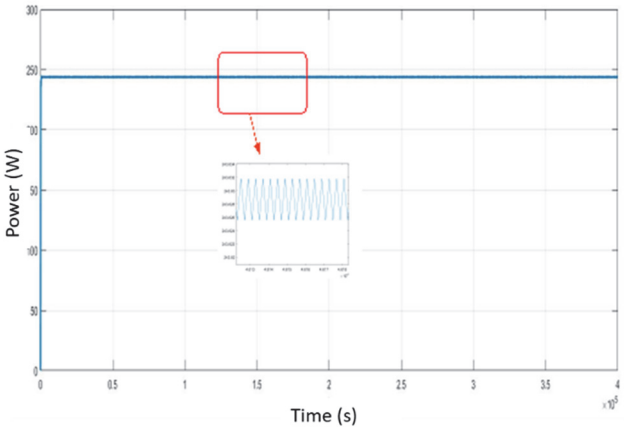

Figure 10 PV power variation over time with the proposed controller applied

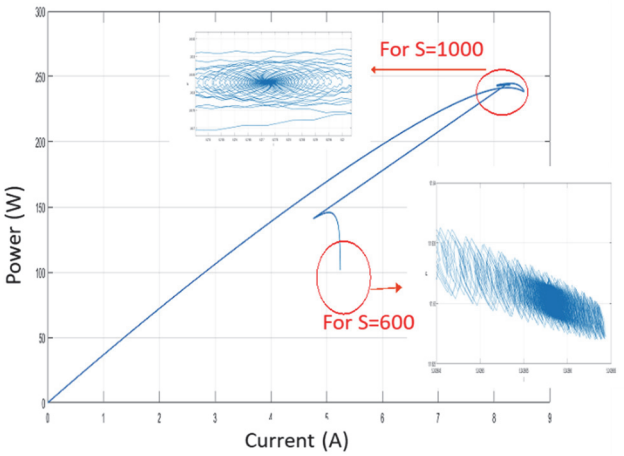

Figure 11 Current-power (*I-P*) characteristic curve of the PV panel for irradiance levels S = 1000 W/m² and S = 600 W/m² under the proposed controller

The change in power of PV controlled with the proposed controller over time is as shown in Fig. 12.

The current-power (*I-P*) graph of the PV for the temperature values T = 25 °C and T = 50 °C, controlled by the proposed controller, is as shown in Fig. 13.

The results in this study come from deterministic simulations rather than repeated experiments, so traditional statistical tools like error bars or confidence intervals are not directly applicable. Instead, to strengthen the evaluation of robustness and repeatability, we carried out additional simulations under different environmental conditions.

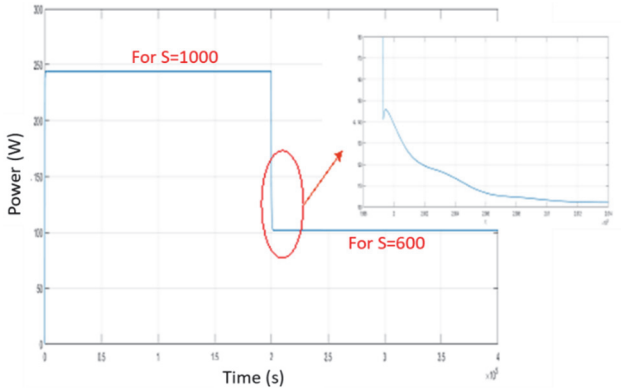

Figure 12 Time-power (*t-P*) response of the PV system at irradiance levels S = 1000 W/m² and S = 600 W/m² under the proposed controller

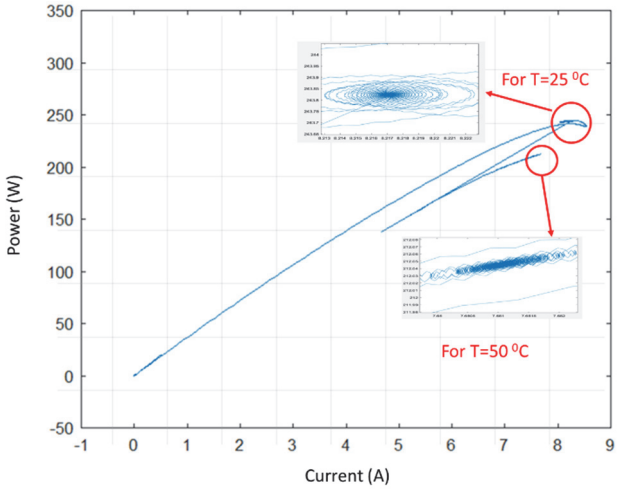

Figure 13 Current-power (*I-P*) characteristic curve of the PV panel for temperature levels T = 25 °C and T = 50 °C under the proposed controller

The measured output power ripple values for these scenarios are presented and discussed in Section 5. The proposed PI-based ESC controller demonstrated that it can operate reliably even with realistic changes in PV system operating conditions, providing consistently stable performance across all tested conditions.

5 CONCLUSION

The current-power (*I-P*) graph of the PV panel output is depicted in Fig. 7. According to Fig. 7, the PV panel has been operated at maximum power using the ES method. It is clearly seen in Fig. 7 that it continuously oscillates around 245 W and exhibits a snail-like movement. Fig. 8 illustrates the time-power graph of the PV panel output. According to Fig. 8, ripple is observed within a range of 0.8 W. Fig. 9 presents the current-power (*I-P*) graph of the PV controlled with the proposed controller. When comparing Fig. 7 and Fig. 9, it can be observed that while there are significant oscillations around the maximum power in the system using only the ESC algorithm in Fig. 7, there are fewer oscillations in Fig. 9. Additionally, in Fig. 9, the maximum power is reached more quickly. Fig. 10 illustrates the power variation of the PV system with the proposed controller applied over time. Comparing Fig. 8 and Fig. 10, it is observed that there is a ripple within a

range of 0.006 W in Fig. 10. This indicates that the new controller has reduced the ripple by 99.25%, which is a very good result. Other studies in the literature generally aim to reduce ripples by 30-70%, therefore the presented results provide a significant advantage in terms of efficiency and system stability. In Fig. 11, the current-power (*I-P*) graph of the PV controlled with the proposed controller is examined by varying the radiation values to $S = 1000$ and $s = 600$. The purpose of examining the radiation change is to test whether the proposed controller quickly finds the maximum power and oscillates around the maximum power during radiation change, and successful results have been obtained. The improved controller responds quickly to sunlight changes and finds the maximum power point more quickly. This shows that the slow adaptation times seen in previous studies have been overcome. While other studies in the literature generally take longer times to find the maximum power, this time has been significantly shortened in this study. Fig. 12 presents the representation of the *I-P* graph from Fig. 11 on the *t-P* graph. In conclusion, the proposed PI-based ESC controller has provided very good results for reducing ripple in the time-power (*t-P*) graph. These ripples are seen as a spiral on the *I-P* graph. In this study, it was observed that the spiral shape in the *I-P* graph became less frequent as the ripples in the *t-P* graph decreased. The *I-P* graphs obtained in this study provide a detailed analysis in terms of reducing ripples. While most studies only examine ripples over *t-P* graphs [22, 33, 34], this study also reveals the spiral formation of *I-P* graphs. The observation that this spiral shape decreases better explains the effectiveness of the control algorithm.

6 REFERANCES

[1] Mamizadeh, A., Mustafa, B. A., & Genc, N. (2021). Planar Flyback Transformer Design for PVPowered LED Illumination. *International Journal of Renewable Energy Research*, *11*(1), 439-445. https://doi.org/10.20508/ijrer.v11i1.11695.g8155

[2] Benda, V. & Cerna, L. (2020). PV cells and modules -State of the art, limits and trends. *Heliyon*, *6*(12), e05666. https://doi.org/10.1016/j.heliyon.2020.e05666

[3] Celik, M. A., Genc, N., & Uzmus, H. (2022). Experimental verification of interleaved hybrid DC/DC boost converter. *Journal of Power Electronics*, *22*, 1665-1675. https://doi.org/10.1007/s43236-022-00471-5

[4] Kart, S., Demir, F., Kocaarslan, İ., & Genc, N. (2024). Increasing PEM fuel cellperformance via fuzzy-logic controlled cascaded DC-DC boost converter. *International Journal of Hydrogen Energy*, *54*, 84-95. https://doi.org/10.1016/j.ijhydene.2023.05.130

[5] Xu, S., Gao, Y., & Zhou, G. (2020). A Global Maximum Power Point Tracking Algorithm for Photovoltaic Systems Under Partially Shaded Conditions Using Modified Maximum Power Trapezium Method. *IEEE Transactions on Industrial Electronics*, *68*(1), 370-380. https://doi.org/10.1109/TIE.2020.2965498

[6] Haji, D. & Genc, N. (2020). Dynamic Behaviour Analysis of ANFIS Based MPPT Controller for Standalone Photovoltaic Systems. *International Journal of Renewable Energy Research*, *10*(1), 101-108.

[7] Balakishan, P., Chidambaram, I. A., & Manikandan, M. (2023). An ANN Based MPPT for Power Monitoring in Smart Grid using Interleaved Boost Converter. *Tehnički vjesnik*, *30*(2), 381-389. https://doi.org/10.17559/TV-20220820194302

[8] Romdlony, Z. R., Trilaksono, B. R., & Ortega, R. (2012). Experimental study of extremum seeking control for maximum power point tracking of PEM fuel cell. *2012 International Conference on System Engineering and Technology*, 5. https://doi.org/10.1109/ICSEngT.2012.6339313

[9] Nedumgatt, J. J., Umaskanhar, S., Vijayakumar, D., & Kothari, D. P. (2011). Perturb and observe MPPT algorithm for solar PV systems-modelling and simulation.*2011 Annual IEEE India Conference*. https://doi.org/10.1109/INDCON.2011.6139513

[10] Thesis-Akihiro, O. (2005). Design and simulation of photovoltaic water pumping system. *California Polytechnic State University*.

[11] Zhong, Z. (2007). Adaptive maximum power point tracking control of fuel cell power plant. *Journal of Power Sources*, *176*(1), 259-269. https://doi.org/10.1016/j.jpowsour.2007.10.080

[12] Hussain Basha, H. & Rani, C. (2020). Different Conventional and Soft Computing MPPT Techniques for Solar PV Systems with High Step-Up Boost Converters: A Comprehensive Analysis. *Energies*, *13*(2), 371. https://doi.org/10.3390/en13020371

[13] Shaw, P. (2019). Modelling and analysis of an analogue MPPT-based PV battery charging system utilising DC-DC boost converter. *IET Renewable Power Energy*, *13*(11), 1958-1967. https://doi.org/10.1049/iet-rpg.2018.6273

[14] Zdiri, M., A., Khelifi, B., Salem, F. B., & Abdallah, H., H. (2021). A Comparative Study of Distinct Advanced MPPT Algorithms for a PV Boost Converter. *International Journal of Renewable Energy Research*, *11*(3), 1156-1165.

[15] Bakar Siddique, M. A., Asad, A., Asif, R. M., Rehman, A. U., Sadiq, M. T., & Ullah, I. (2023). Implementation of incremental conductance MPPT algorithm with integral regulator by using boost converter in grid-connected PV array. *IETE Journal of Research*, *69*(6), 3822-3835. https://doi.org/10.1080/03772063.2021.1920481

[16] Javed, S. &Ishaque, K., A. (2022). A comprehensive analysis with new findings of different PSO variants for MPPT problem under partial shading. *Ain Shams Engineering Journal*, *5*(13), 101680. https://doi.org/10.1016/j.asej.2021.101680

[17] Firdaus, A. A., Yunardi, R. T., Agustin, E. I., Nahdliyah, S. D. N., & Nugroho, T. A. (2020). An improved control for MPPT based on FL-PSO to minimize oscillation in photovoltaic system. *International Journal of Power Electronics and Drive System (IJPEDS)*, *2*(11), 1082-1087. https://doi.org/10.11591/ijpeds.v11.i2.pp1082-1087

[18] Vaigundamoorthi, M., Ramesh, R., Vasan Prabhu, V., & Arul Kumar, K. (2020). MPPT oscillations minimization in PV system by controlling non-linear dynamics in SEPIC DC-DC converter. *International Journal of Electrical and Computer Engineering (IJECE)*, *6*(10), 6268-6275. https://doi.org/10.11591/ijece.v10i6.pp6268-6275

[19] Brunton, S. L., Rowley, C. W., Kulkarni, S. R., & Clarkson, C. (2010). Maximum Power Point Tracking for Photovoltaic Optimization Using Ripple-Based Extremum Seeking Control. *IEEE Transactions on Power Electronics*, *25*(10), 2531-2540. https://doi.org/10.1109/TPEL.2010.2049747

[20] Zazo, H., Del Castillo, E., Reynaud, J. F., & Leyva, R. (2012). MPPT for Photovoltaic Modules via Newton-Like Extremum Seeking Control. *Energies*, *5*(8), 2652-2666. https://doi.org/10.3390/en5082652

[21] Ghaffari, A., Krstić, M., & Seshagiri, S., (2014). Power Optimization for Photovoltaic Microconverters Using Multivariable Newton-Based Extremum Seeking. *IEEE Transactions on Control Systems Technology*, *22*(6), 2141-2149. https://doi.org/10.1109/TCST.2014.2301172

[22] Chellakhi, A. A., El Beid, S., & Abouelmahjoub, Y. (2022). An Advanced MPPT Scheme for PV Systems Application

with Less Output Ripple Magnitude of the Boost Converter. *International Journal of Photoenergy*, *2022*(1), 133294. https://doi.org/10.1155/2022/2133294

[23] Atallah, A. M., Abdelaziz, A. Y., & Jumaah, R. S. (2014). Implementation of Perturb and Observe Mppt of PV System with Direct Control Method Using Buck and Buck-Boost Converters. *Emerging Trends in Electrical, Electronics & Instrumentation Engineering: An international Journal (EEIEJ)*, *1*(1).

[24] Freitas, A. A. A., Tofoli, F. L., Junior, E. M. et al. (2016). Analysis of high voltage step-up nonisolated DC-DC boost converters. *International Journal of Electronics*, *103*(5), 898-912. https://doi.org/10.1080/00207217.2015.1077529

[25] Rensburg, J. V., Case, M. J., & Nicolae, D. V. (2008). Double-boost DC to DC converter. *Industrial Electronics IECON. 34th Annual Conference of IEEE*, 707-711. https://doi.org/10.1109/IECON.2008.4758040

[26] Genc, N. & Koc, Y. (2017). Experimental verification of an improved soft-switching cascade boost converter. *Electric Power Systems Research*, *149*, 1-9. https://doi.org/10.1016/j.epsr.2017.04.015

[27] Kocaarslan, I., Kart, S., Genc, N., & Uzmus, H. (2019). Design and application of PEM fuel cell-based cascade boost converter. *Electrical Engineering*, *101*, 1323-1332. https://doi.org/10.1007/s00202-019-00871-0

[28] Liu, G., Zhu, L., Li, H., Li, J., & Lv, Q. (2023). Novel extreme seeking control framework with ordered excitation and nonlinear function based PSO: Method and application. *Solar Energy*, *25*(5), 126-137. https://doi.org/10.1016/j.solener.2023.03.030

[29] Moura, S. J. & Chang, Y. A. (2013). Lyapunov-based switched extremum seeking for photovoltaic power maximization. *Control Engineering Practice*, *21*(7), 971-980. https://doi.org/10.1016/j.conengprac.2013.02.009

[30] Anandanatarajan, R., Chidambaram, M., & Jayasingh, T. (2006). Limitations of a PI controller for a first-order nonlinear process with dead time. *ISA transactions*, *45*(2), 185-199. https://doi.org/10.1016/S0019-0578(07)60189-X

[31] Gupta, M., Tiwari, P. M., Viral, R. K. et al. (2025). Grid-connected PV inverter system control optimization using Grey Wolf optimized PID controller. *Scientific Reports*, *15*, 28869. https://doi.org/10.1038/s41598-025-10617-7

[32] Chellakhi, A., El Beid, S., & Abouelmahjoub, Y. (2020). Ripples Amplitude Minimizing of the Output Boost Converter Using an Innovative MPPT Controller for PV Systems Applications. *2020 IEEE 2nd International Conference on Electronics, Control, Optimization and Computer Science (ICECOCS)*. https://doi.org/10.1109/ICECOCS50124.2020.9314628

[33] Abu Taher, M., Behnamfar, M., Sarwat, A. I., & Tariq, M. (2024). Wavelet and Signal Analyzer Based High-Frequency Ripple Extraction in the Context of MPPT Algorithm in Solar PV Systems. *IEEE Access*, *12*, 113726-113740. https://doi.org/10.1109/ACCESS.2024.3426289

Contact information:

Sude KART, Dr
Karabuk University,
Department of Electric and Energy,
Karabuk, Turkey
E-mail: sudekart@karabuk.edu.tr